Structural studies of two protonated forms of a C_2 symmetrical optically active cyclam derivative

Ignacio Alfonso,[a] Covadonga Astorga,[a] Francisca Rebolledo,*[a] Vicente Gotor,*[a] Santiago García-Granda[b] and Ana Tesouro[b]

[a] *Departamento de Química Orgánica e Inorgánica, Universidad de Oviedo, 33071 Oviedo, Spain*
[b] *Departamento de Química Física y Analítica, Universidad de Oviedo, 33071 Oviedo, Spain*

Received (in Cambridge, UK) 22nd June 1999, Accepted 24th December 1999
Published on the Web 9th March 2000

Detailed structural analyses, including solid-state (X-Ray), solution-state (NMR) and theoretical (AM1) studies of the two most stable protonated forms — di $\mathbf{3H_2}^{2+}$ and tetraprotonated $\mathbf{3H_4}^{4+}$ — of a C_2 symmetrical, optically active cyclam derivative **3** have been carried out. Important conformational changes in the 14-membered and cyclohexane rings accompany the protonation. A rigid conformation with C_2 symmetry stabilized by bifurcated intramolecular hydrogen bonds is obtained for $\mathbf{3H_2}^{2+}$, whereas for $\mathbf{3H_4}^{4+}$ a dynamic system in solution and a loss of the C_2 symmetry in the solid state are found. The effects of temperature and the counter-ion are also discussed.

Introduction

Cyclam (1,4,8,11-tetraazacyclotetradecane) is perhaps one of the most useful azamacrocycles due to its ability to act as effective metal-ion binding site and also its basic properties.[1] Structural changes, like the presence of methyl groups on N and C positions in the cyclam structure, or the incorporation of functionalized substituents, lead to changes in the metal binding behavior of the macrocycle as well as in their protonation capability.[2] Some of these differences have been explained in terms of the modification of coordination geometry and, therefore, of ring conformation.[3] Taking into account the close relation between conformation and some properties of cyclam derivatives, it is surprising that most of the studies on these compounds have been performed in solid-state[4] in combination with molecular modeling calculations,[5] while data concerning the structures in solution are very scarce.[6]

In a recent paper we have described the synthesis of some optically active cyclam analogs.[7] Thus, starting from (*S*,*S*)-cyclohexane-1,2-diamine [(*S*,*S*)-**1**] or from tetraamine (*R*,*R*)-**2**, both enantiomers of the C_2 symmetrical cyclam derivative (*S*,*S*)- or (*R*,*R*)-**3** have been prepared. Because of the scarcity of structural studies about cyclam and its derivatives, we consider a structural study of this C_2 symmetrical cyclam analog at different protonation degrees, to be of interest. This study covers the solid-state, solution-state and calculated structures of the two most stable protonated forms of **3**, the di- and tetraprotonated species.

Experimental and theoretical methods

X-Ray crystallographic analysis †

Salt (*R*,*R*)-$\mathbf{3H_2}^{2+}(ClO_4)_2^{2-}$ is formed by mixing equimolecular amounts of (*R*,*R*)-$\mathbf{3H_4}^{4+}(ClO_4)_4^{4-}$ and (*R*,*R*)-**3**, and it crystallizes from a methanol–water mixture as colorless needles.

The salt (*S*,*S*)-$\mathbf{3H_4}^{4+}\mathbf{Br_4}^{4-}$ crystallizes from a 48% aq HBr–ethanol mixture as colorless needles.

Crystal data and refinement parameters for the two structures, $\mathbf{3H_2}^{2+}(ClO_4)_2^{2-}$ and $\mathbf{3H_4}^{4+}\mathbf{Br_4}^{4-}$, are shown in Table 1. The unit-cell dimensions were determined from the angular settings of 25 reflections with θ between 13/7 and 15°. The space groups were determined to be $P2_1/P1$, both from systematic absences and from the structural determination. The intensity data sets were measured using the ω–2θ scan technique and a variable scan rate, with a maximum scan time of 60 s per reflection. The intensity of the primary beam was checked throughout the data collection by monitoring three standard reflections every 60 min. The final drift correction factors were between 0.991/0.957 and 1.038/1.025. A profile analysis was performed on all reflections.[8] Some double measured reflections were averaged, $R_{int} = \Sigma I - \langle I \rangle / \Sigma I$. Lorentz and polarization corrections were applied and the data were reduced to F_o^2 values. The structure of $\mathbf{3H_4}^{4+}\mathbf{Br_4}^{4-}$ was solved by Patterson methods and phase expansion using DIRDIF,[9] while the structure of $\mathbf{3H_2}^{2+}(ClO_4)_2^{2-}$ was solved directly by SHELXS86.[10] Isotropic least-squares refinement on F^2 was made using SHELXL93.[11] At this stage an empirical absorption correction was applied using XABS2.[12] The relative maximum and minimum transmission factors were 0.1693/0.575 and 1.000/1.000, respectively.

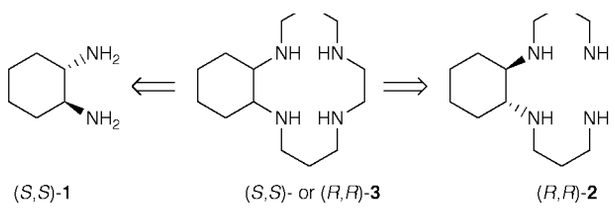

Scheme 1 Retrosynthesis of (*S*,*S*)- or (*R*,*R*)-**3**.

During the final stages of the refinement the positional parameters and the anisotropic thermal parameters of the non-H atoms were refined. All non-hydrogen atoms were anisotropically refined. Hydrogen atoms attached to all carbon atoms were found by low angle difference Fourier synthesis, but due to their lack of stability they were refined riding from the ideal geometry using common thermal parameters. Most of H-atoms bonded to nitrogens were also located by difference Fourier synthesis. Water H-atoms were fixed and refined taking the oxygen thermal parameter as reference.

For structure $\mathbf{3H_2}^{2+}(ClO_4)_2^{2-}$, atom C(28) was isotropically refined and atom O(34) was found split into two very close positions and was anisotropically refined.

The minimized function was $[\Sigma w(F_o^2 - F_c^2)2/\Sigma w(F_o^2)^2]^{1/2}$, $w = 1/[\sigma^2(F_o^2) + (0.0274P)^2 + 10.09P]$ with $\sigma(F_o^2)$ from count-

* E-mail: vgs@sauron.quimica.uniovi.es
† CCDC reference number 188/214. See http://www.rsc.org/suppdata/p2/a9/a904998c for crystallographic files in .cif format.

DOI: 10.1039/a904998c

Table 1 Crystal data and structure refinement for $3H_4^{4+}Br_4^{4-}$ and $3H_2^{2+}(ClO_4)_2^{2-}$

Identification codes	$\mathbf{3}H_4^{4+}Br_4^{4-}$	$\mathbf{3}H_2^{2+}(ClO_4)_2^{2-}$
Empirical formula	$C_{14}H_{36}Br_4N_4O$	$C_{14}H_{32}C_{12}N_4O_8$
Formula weight	596.11	455.34
Temperature/K	293(2)	
Wavelength/Å	0.71073	
Crystal system	Monoclinic	Triclinic
Space group	$P2_1$	$P1$
Unit cell dimensions		
a/Å, α/°	7.990(10)	8.033(6)/100.01(6)
b/Å, β/°	15.168(2), 106.69(6)	8.268(7)/94.67(5)
c/Å, γ/°	9.713(1)	18.03(2)/116.89(7)
Volume/Å^3	1128(1)	1034(2)
Z	2	2
Density (calculated)/mg m^{-3}	1.756	1.462
Absorption coefficient/mm^{-1}	7.147	0.363
F(000)	592	484
Crystal size/mm^3	0.26 × 0.13 × 0.07	0.23 × 0.10 × 0.07
θ range/°	2.19–24.98	1.17–25.00
Index ranges	$-9 \leqslant h \leqslant 9$, $-1 \leqslant k \leqslant 18$, $0 \leqslant l \leqslant 11$	$-9 \leqslant h \leqslant 9$, $-9 \leqslant k \leqslant 9$, $0 \leqslant l \leqslant 21$
Reflections collected	2378	3765
Independent reflections	2233 [R(int) = 0.079]	3639 [R(int) = 0.0812]
Refinement method	Full-matrix least-squares on F2	
Data/restraints/parameters	2233/10/253	3765/22/533
Goodness-of-fit on F^2	1.037	1.008
Final R indices [$I > 2\sigma(I)$]	$R1 = 0.0467$, $wR2 = 0.0971$	$R1 = 0.0581$, $wR2 = 0.1207$
R indices (all data)	$R1 = 0.1450$, $wR2 = 0.1320$	$R1 = 0.2101$, $wR2 = 0.1689$
Absolute structure parameter	0.02(5)	
Largest diff. peak and hole/e Å^{-3}	0.783 and −1.078	0.395 and −0.437

ing statistics and $P = (\mathrm{Max}(F_o^2,O) + 2*F_c^2)/3$, for $\mathbf{3}H_4Br_4$, and $w = 1/[\sigma^2(F_o^2) + (0.0599P)^2]$ for $\mathbf{3}H_2(ClO_4)_2$. The crystallographic plots were made by a EUCLID package.[13]

Atomic scattering factors were taken from International Tables for X-ray Crystallography.[14] Geometrical calculations were made with PARST.[15] All calculations were made at the University of Oviedo on the Scientific Computer Center and X-Ray group DEC/AXP-computers.

NMR experiments

NMR spectra were run on Brucker AC200, AC300 and AMX400 spectrometers. Selected spectral parameters were as follows. ^1H,^{13}C 2D HMQC[16] spectral width, 2008 Hz in F2 and 5534 Hz in F1 for $\mathbf{3}H_2^{2+}$, 1760 Hz in F2 and 6850 Hz in F1 for $\mathbf{3}H_4^{4+}$; 128 increments recorded; final matrix after zero filling, 2048 × 256; evolution delay of $^1J_{CH}$, 2.45 ms; 16 scans per increment in F1. The same parameters were used for the corresponding ^1H,^{13}C 2D HMBC[16] spectra. In these experiments the number of scans was 32 and the evolution delay of $^nJ_{CH}$ was set to 60 ms. 2D ROESY:[16] 3125 Hz for $\mathbf{3}H_2^{2+}$ and 2263 Hz for $\mathbf{3}H_4^{4+}$, all of them in both dimensions; 128 increments recorded; final matrix after zero filling, 2048 × 256; spin-lock mixing time 200 ms; spin-lock field $\gamma B_1/2\pi \simeq 4.5$ kHz 40 scans per increment in F1. All the spectra were acquired in the TPPI mode, and a shifted sinus bell multiplication of π/2 in both dimensions prior to transformation was performed.

Theoretical calculations

Solid state structures, from experimental X-ray diffraction, were used as starting geometries when available. In the other cases, a preliminary conformational searching was performed with the MMX force field as implemented in PCMODEL[17] program. The structures thus obtained were used as starting geometries for the semiempirical AM1[18] level of theory in the Gaussian94 program. They were fully minimized without symmetry constraints and the frequencies analysis showed they were minima of energy.

Results and discussion

Both for crystallization and for NMR analyses of the diprotonated and tetraprotonated species of **3**, the almost exclusive

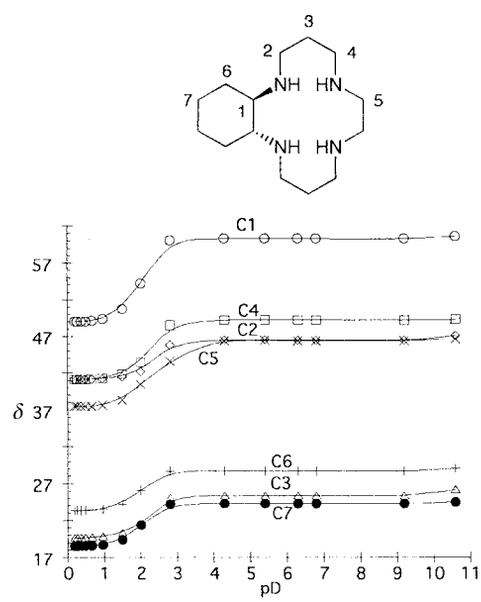

Fig. 1 Change in δ_C with pD for 100 mg (*R*,*R*)-**3** in 1 ml D_2O, pH adjusted with aq. HBr.

presence of each species in solution is advisable. This requires an adequate control of the pH value. By means of ^{13}C-NMR spectroscopy,[19] we have carried out an analysis of the degree of protonation of (*R*,*R*)-**3** in D_2O at different acid concentrations. Samples were prepared with (*R*,*R*)-**3** (100 mg) and D_2O (1 mL) adjusting the pH value with concentrated aqueous HBr. The results obtained are shown in Fig. 1.

Each line represents the variation of experimental chemical shift for each carbon atom in the pD range 11–0.2.[20] All the carbon signals shift to higher field when the degree of protonation increases.[19] The two straight sections, at pD between 9–4.5 and at pD < 0.8, have special significance, suggesting the presence of a major species in every section. By comparison with the pKa$_a$ values measured for cyclam (pK_{a1} = 11.6, pK_{a2} = 10.6, pK_{a3} = 1.61, pK_{a4} = 2.42)[5b] and taking into account that pK_{a1} and pK_{a2} are not significantly affected by C-alkylation,[21] it seems clear that the diprotonated species ($\mathbf{3}H_2^{2+}$) is the major

Table 2 Selected experimental (X-ray) and calculated (AM1) geometrical data for $3H_2^{2+}(ClO_4)_2^{2-}$ and for $3H_4^{4+}Br_4^{4-}$ (intramolecular N–N distances in Å, torsion angles in degrees)

	$3H_2^{2+}(ClO_4)_2^{2-}$			$3H_4^{4+}Br_4^{4-}$	
	Exp. 1	Exp. 2	Calc.	Exp.	Calc.
N(1)–N(2)	2.85(1)	2.85(2)	2.92	3.73(2)	3.84
N(3)–N(4)	2.89(1)	2.92(2)	2.98	3.18(2)	3.24
N(2)–N(3)	2.86(2)	2.92(1)	3.09	4.27(2)	4.42
N(1)–N(4)	2.92(2)	2.87(1)	3.08	4.48(2)	4.59
N(1)–N(3)	4.09(2)	4.10(2)	4.31	5.78(2)	5.83
N(2)–N(4)	4.06(2)	4.07(2)	4.23	5.23(2)	5.50
N(1)–C(1)–C(6)–N(2)	−59.0(1)	−56.0(1)	−51	160.0(2)	164
N(3)–C(10)–C(11)–N(4)	−61.0(2)	−63.0(2)	60	−70.0(2)	68
N(2)–C(7)–C(8)–C(9)	−66.0(2)	66.0(2)	77	59.0(2)	62
C(7)–C(8)–C(9)–N(3)	−65.0(2)	−63.0(2)	−68	−163.0(2)	−161
N(4)–C(12)–C(13)–C(14)	−68.0(2)	−68.0(2)	−74	−76.0(2)	−79
C(12)–C(13)–C(14)–N(1)	−67.0(2)	64.0(2)	71	173.0(2)	177

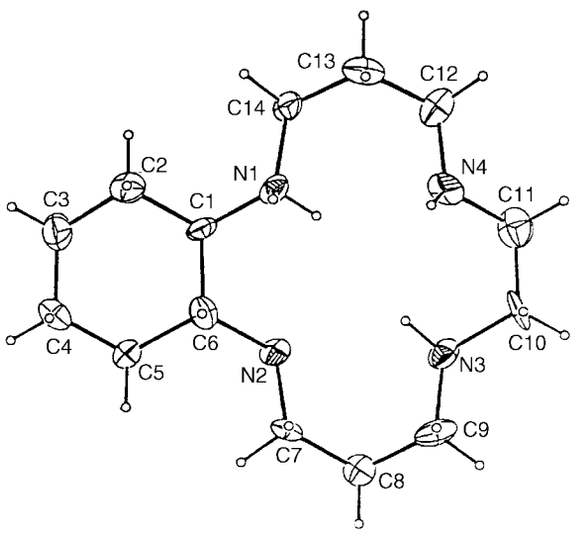

Fig. 2 One of the two conformations of the cation in solid state (*R*,*R*)-$3H_2^{2+}(ClO_4)^{2-}$.

species at pD 9–4.5, and the tetraprotonated ($3H_4^{4+}$) is the main species at pD < 0.8. Moreover, the width of the first section discloses a great difference between pK_{a2} and pK_{a3} values for our macrocycle, such as is shown for cyclam. By means of MM calculations[5b] this difference was explained for cyclam in terms of conformational changes. A more detailed study of solid-state, solution-state and calculated gas-state structures of $3H_2^{2+}$ and $3H_4^{4+}$ is shown below.

Structural analysis of (*R*,*R*)-$3H_2^{2+}(ClO_4)_2^{2-}$

The solid state conformation was determined by X-ray analysis (Fig. 2). The asymmetric unit consists of two macrocyclic cations and four perchlorate anions. Both cations possess similar, but not identical, conformations. Fig. 2 offers a view of the molecular structure of one of the two macrocyclic cations, the numbering scheme stemming from the X-ray crystallographic results. Selected bond distances and torsion angles are given in Table 2.

The cyclohexane ring adopts a chair conformation with both nitrogens [N(1) and N(2)] in equatorial positions. All the C–C units of the 14-membered ring (see Table 2) adopt a *gauche* conformation, both rings being almost coplanar. In order to minimize electrostatic repulsions, protonation takes place on alternate nitrogens [N(1) and N(3)], placing the four nitrogens in *endo* position, and in the same plane (with only 5% of deviation from the ideal least-squares plane through the four N-atoms). This arrangement of the nitrogen atoms, as well as the proximity between them ($N^+ \cdots N$ is below 3.0 Å[22]) favors the formation of bifurcated intramolecular hydrogen bonds.[23] Based on this assumption, all nitrogen atoms within the ring are intramolecularly hydrogen-bonded, forming six-membered and five-membered rings. Torsion angle values for the N–C–C–C–N fragments (see Table 2) are in accordance with a chair-like conformation for the six-membered rings.

Both perchlorate anions are placed over and on the underside of the mean macrocyclic plane. The shortest $N \cdots O$ distances are within the range expected for the type oxy anion-to-NH hydrogen bond,[24] and are applicable to all the nitrogen atoms.

Solution structure of (*R*,*R*)-$3H_2^{2+}Br_2^{2-}$ in D_2O

The dihydrobromide of (*R*,*R*)-**3** was prepared by dissolving equimolecular amounts of the (*R*,*R*)-$3H_4^{4+}Br_4^{4-}$ and the free amine (*R*,*R*)-**3** in D_2O (pD of the solution = 6.5). ^1H and ^{13}C NMR spectra of (*R*,*R*)-$3H_2^{2+}Br_2^{2-}$ show thirteen and seven signals, respectively, thus revealing an effective C_2 symmetry for the compound in the NMR–time scale (Table 3).

Chemical inequivalence is shown for all the CH_2 protons of both rings. As a general rule, for each CH_2 group the most deshielded proton shows a large coupling constant (assignable to $^2J_{HH}$) and at least two small ones (assignable to two *gauche* couplings), whereas the most shielded proton shows at least two large *J*, which are assignable to $^2J_{HH}$, and to one antiperiplanar coupling. This indicates the presence in solution of one conformer with axial and equatorial positions for all the protons of the molecule, the most deshielded proton being the equatorial.[25] The well-defined axial and equatorial positioning for all the CH_2 protons, suggests a fast prototropic process in the inner cavity of the macrocycle, the protonation sites being averaged between the four nitrogens. Values of the coupling constants for the propylene unit (Table 3) are in accordance with the existence of a pseudo-chair conformation for the six-membered ring, built up at the expense of a strong intramolecular hydrogen bond between nitrogen atoms. In addition, the ROESY spectrum of **3** shows a cross peak between H(2*e*) and H(6*e*), supporting the co-planarity between the six and 14-membered rings. With these data, we propose a conformation similar to both the solid structure and the conformation of the free amine in $CDCl_3$.[7] Semi-empirical calculations with the AM1 Hamiltonian[18] using the X-ray data for the starting geometry leads to an energy minimum in good agreement with the solid-state conformation (Table 2).

In order to study the conformational stability of this compound, ^1H NMR experiments at temperatures in the range 278–358 K were carried out, no significant changes being observed. All these NMR experiments show that the bifurcated intracationic hydrogen bonds of $3H_2^{2+}$ are so strong that they give the structure a rigid conformation in solution, a structure which is retained even at 358 K.

Table 3 ^{1}H and ^{13}C NMR data for $3H_2^{2+}Br_2^{2-}$ and for $3H_4^{4+}Br_4^{4-}$ (in D_2O)

	$3H_2^{2+}Br_2^{2-}$			$3H_4^{4+}Br_4^{4-}$	
Position[a]	δ_{He} (*J*/Hz)	δ_{Ha} (*J*/Hz)	δ_C	δ_H[b]	δ_C
1	—	2.65 m	60.3	3.92	49.0
2	3.36 ddd (−12.2, 4.0, 2.9)	2.73 ddd (−12.2, 9.6, 4.7)	46.5	3.23	41.1
3	1.93 m (−13.4, 5.3, 4.7, 4.1, 4.0)	1.93 m (−13.4, 9.6, 9.3, 2.9, 2.9)	25.4	1.94	19.7
4	3.12 ddd (−11.6, 4.1, 2.9)	2.94 ddd (−11.6, 9.3, 5.3)	49.3	3.23	41.1
5	3.07 qAB	2.88 qAB	46.4	3.41	37.5
6	2.27 m	1.10 m	28.7	1.72	23.3
7	1.75 m	1.20 m	24.3	1.49/1.31	18.5

[a] Numbering as is shown in Fig. 1. [b] Broad signals for all the protons.

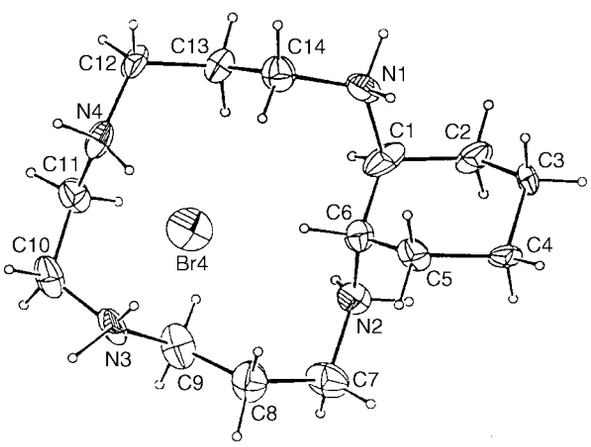

Fig. 3 Molecular structure of the (*S*,*S*)-$3H_4^{4+}Br_4^{4-}$ cation.

Introduction of a metal-ion (Fe^{2+}, Ni^{2+}, *etc.*) in the inner cavity of **3** would occupy the position of the two endo protons in $3H_2^{2+}$, leading to an optically active complex. This will be of great importance for the further application of **3** complex derivatives as potential catalysts in asymmetric synthesis.

Structural analysis of (*S*,*S*)-$3H_4^{4+}Br_4^{4-}$

A view of the molecular structure of the cation with the numbering scheme adopted is shown in Fig. 3.

The cyclohexane ring adopts a chair conformation with a diaxial arrangement of the N(1) and N(2) ammonium groups [torsion angle N(1)–C(1)–C(6)–N(2) of 160.(2)°], thus avoiding electrostatic repulsions. An important structural characteristic of the 14-membered ring is the proximity of the Br(4) bromide anion to both the N(3) and N(4) ammonium groups. The interionic distances, Br(4)···N(3) of 3.26(2) Å and Br(4)···N(4) of 3.30(1) Å, are less than the sum of van der Waals radii of Br and N (*ca.* 3.40 Å),[22] supporting the existence of hydrogen bonding between Br(4) and both H(31)–N(3) and H(42)–N(4).[23] These bonding interactions contribute to stabilize the *gauche* arrangement adopted by the N(3) and N(4) ammonium groups [torsion angle N(3)–C(10)–C(11)–N(4) of −70.(2)°] in contrast with the N(1) and N(2) groups. As a consequence, the cation adopts a different conformation to that of C_2 symmetry, and both N–C–C–C–N frameworks adopt a conformation placing the cyclohexane ring nearer to C(7) [torsion angle C(7)–N(2)–C(6)–C(5) of 56.(2)°] than to C(14) [torsion angle C(14)–N(1)–C(1)–C(2) of 180.(2)°].

In order to obtain information about the conformation of the tetraprotonated macrocycle in solution, the salt was dissolved in D_2O and 48% HBr was added until pD = 0.2. The ^{13}C NMR spectrum (Table 2) consists of seven signals, meaning that $3H_4^{4+}$ presents an averaged conformation with C_2 symmetry in solution. The ^{1}H NMR spectrum (Table 2) shows broad signals for all the protons, thus indicating the existence of a conformationally mobile system. Diastereotopic CH_2 protons are indistinguishable (298 K), except for those of C(7) [two

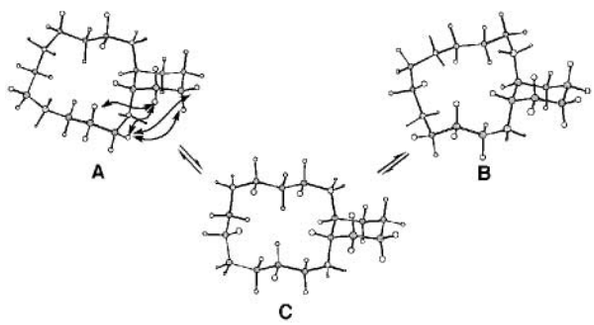

Fig. 4 Conformations of (*S*,*S*)-$3H_4^{4+}Br_4^{4-}$ in solution **A** is that of the solid state cation.

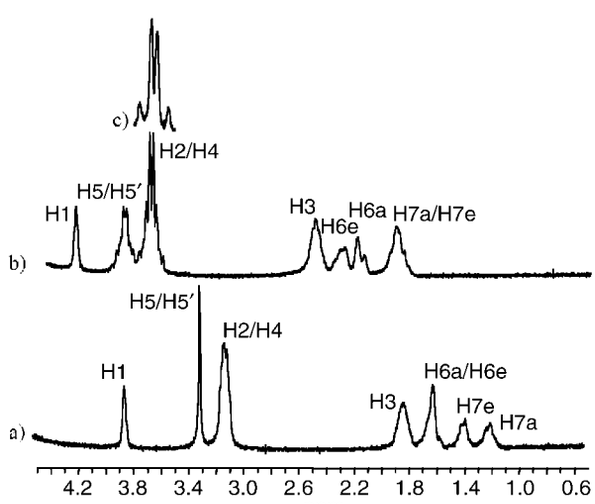

Fig. 5 ^{1}H NMR of (*S*,*S*)-$3H_4^{4+}Br_4^{4-}$ (a) at 278 K, (b) at 333 K. (c) Shows the second-order multiplet for H(2)/H(2′)/H(4)/H(4′) simplified to an AB quartet on irradiation of the H(3)/H(3′) signal.

resonances at 1.31 (H(7*a*)) and 1.49 (H(7*e*)) ppm]. H(5) forms an A_2 spin system and a broad signal is assigned to H(2)/H(4) protons. H(1) resonates at 3.92 ppm and it is the lowest–field signal of the spectrum. These data suggest that the cyclohexane ring of $3H_4^{4+}$ is locked in a chair conformation with H(1) in the equatorial position.[25] ROESY spectrum[16] shows cross peaks of H(1) with H(2) (and/or H(4)) and H(3), supporting an *endo* position of H(1) (towards the inner part of the 14-membered ring). Moreover, the ROEs observed in this spectrum also indicate that the solid-state structure **A** (Fig. 4) of $3H_4^{4+}$ is retained in solution. Because C_2 symmetry is necessary, structure **A** must be in equilibrium with at least another structure, such as **B**, which only differs from **A** in the 14-membered ring conformation.

The analysis of the ^{1}H NMR spectra at different temperatures shows no significant changes in the range 278 (Fig. 5a)–313 K. However, at 333 K the changes are important (Fig. 5b), most of the diastereotopic CH_2 protons being distinguishable.

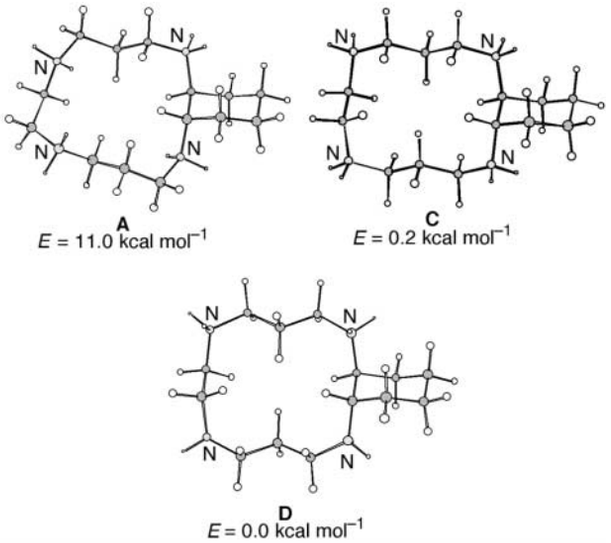

Fig. 6 Energy minima found by AM1 calculation on (*S*,*S*)-$\mathbf{3H_4}^{4+}$.

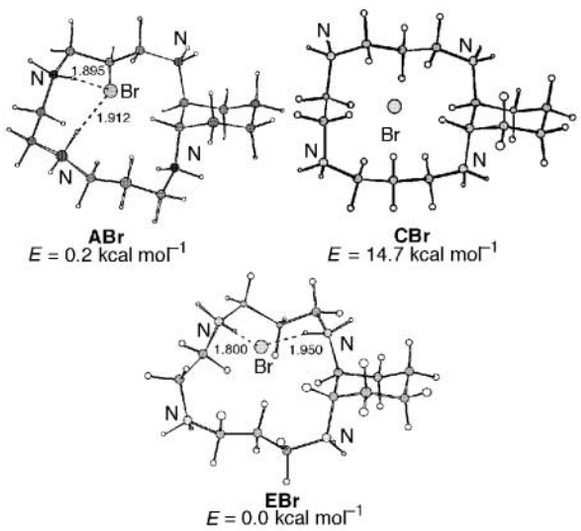

Fig. 7 Effect of counterion on minima shown in Fig. 6. Conformation **D** becomes **E**Br.

H(5) and H(5′) form an AA′BB′ system at 3.93 ppm; H(2) and H(2′) show the same chemical shifts as H(4) and H(4′), respectively, appearing as a second-order multiplet (centered at 3.74 ppm), which is simplified to an AB quartet (J_{AB} = 13.6 Hz) when the signal of H(3)/H(3′) (2.52 ppm) is irradiated (Fig. 5c). H(1) is still the most de-shielded proton (4.29 ppm), and H(7*e*) and H(7*a*) coalesce at 1.93 ppm, whereas H(6*e*) and H(6*a*) show two signals at 2.35 and 2.20 ppm, respectively. These data are in agreement with a fully alternated conformation **C**, which presents both C_2 symmetry and an *anti* arrangement of all the ammonium groups. Although **C** structure is not consistent with some ROE's observed at room temperature, it could be present at $T < 333$ K given that **C** is the intermediate conformation necessary to convert **A** into **B** (Fig. 4). In addition to this, when temperature is raised over 333 K, the signals of the spectrum become broader, so their chemical inequivalence disappears. This fact suggests that the proposed rigid conformation **C** is broken at $T > 333$ K.

In order to rationalize these conformational changes, we have chosen a theoretical (AM1) approach. Three energy minima, **A** (very close to the solid-state structure), and **C** and **D** with an *anti* arrangement for the ammonium groups, are obtained. Both **C** (10.8 kcal mol^{-1}) and **D** (11.0 kcal mol^{-1}) proved to be more stable than conformer **A** (Fig. 6), but this stability order disagrees with the conformations found through the temperature-dependent NMR analysis.

Because the driving force for the presence of the less stable **A** conformer in solution could be similar to that in the solid-state, that is, the existence of bonding interactions with the bromide anion,[26] we decided to estimate the effect of the counter-ion by AM1 calculations. To do this, one bromide was placed as found in the crystal for the **A** conformer, and equidistant to the four nitrogen atoms for both **C** and **D**. The minimum obtained for **A**Br$^-$ is 14.5 kcal mol^{-1} lower in energy than for **C**Br$^-$ (Fig. 7). For **D** the presence of the bromide anion leads to a conformational change in one of the propylene units, obtaining a minimum (**E**Br$^-$) in which two ammonium groups are closer. These results imply that bromide stabilization effect is more effective for **A** and **E** conformers than for **C**, probably due to the formation of two strong hydrogen bonds in both **A** and **E** (see Fig. 7). We can conclude that the tetracation–bromide interaction remains in solution at room temperature and the inversion of the 14-membered ring through conformer **E**Br$^-$ is fast in the NMR time scale. When T is increased (333 K), thermal energy breaks the bromide interactions, and the molecule changes to a more stable conformer (**C** or **D**), as is shown by NMR and AM1 calculations of the isolated tetracation.

In addition, the binding effect of the bromide anion in solution was also proved when the ^{1}H NMR spectrum was recorded with a larger counter-ion. Thus, by using H_2SO_4 acid instead of HBr to adjust the pD value, H(5) and H(5′) form a clearly resolved AA′BB′ system compatible with the conformation **C** and similar to the result obtained with HBr at 333 K.

On the other hand, experimental proof of the ion-pair interactions in gas-phase for $\mathbf{3H_4}^{4+}\mathbf{Br_4}^{4-}$ were obtained. Thus, fast atom bombardment mass spectrometry (FABMS)[27] shows two equally intense peaks at *m*/*z* 335 and 337 corresponding to $[\mathbf{3H_2}^{79}\mathrm{Br}]^+$ and $[\mathbf{3H_2}^{81}\mathrm{Br}]^+$, respectively.

The apparently higher binding anion ability of $\mathbf{3H_4}^{4+}$ compared to tetraprotonated cyclam could be explained in terms of poorer solvation of the ammonium sites of $\mathbf{3H_4}^{4+}$ due to their more hydrophobic environment. This exceptional ability of the fused cyclohexane-cyclam can be exploited in the design of other optically active polyammonium macrocycle analogs[28] which can act as receptors of chiral anions.

In summary, an exhaustive study of the diprotonated ($\mathbf{3H_2}^{2+}$) and tetraprotonated ($\mathbf{3H_4}^{4+}$) compounds reveals the conformational changes that accompany protonation. In **3**[7] and $\mathbf{3H_2}^{2+}$ all the nitrogen atoms are placed in *endo*, with a *trans*-diequatorial arrangement of the cyclohexane moiety, a strong similarity between the solution and calculated structures being found. The same structure is obtained in the X-ray analysis of $\mathbf{3H_2}^{2+}(\mathrm{ClO_4}^-)_2$. The driving force for the existence of this common structure is its high stability resulting from strong intramolecular hydrogen bonds.

The solid state structure of $\mathbf{3H_4}^{4+}$ $\mathrm{Br_4}^{4-}$ shows a *trans*-diaxial arrangement for the cyclohexane moiety and a *gauche* disposition for the ethylendiammonium unit, leading to a loss of the C_2 symmetry. This conformation, stabilized by bromide–ammonium groups interactions, is retained in solution, but it is in equilibrium with other conformations, and displays an averaged C_2 symmetry.

Two interesting characteristics could be of great importance for further applications of this compound: (i) the major affinity of compound $\mathbf{3H_4}^{4+}$ for the bromide anion compared with that of cyclam, and (ii) the rigid conformation of the diprotonated species, which implies an efficient transference of chirality throughout the ring.

Further applications of this compound as a chiral tool are currently in progress.

Acknowledgements

This work was supported by the CICYT (BIO-98-0770). I. A. thanks the Ministerio de Educación y Ciencia for a predoctoral fellowship.

References

1 E. Kimura, *Tetrahedron*, 1992, **48**, 6175.

2 (*a*) A. J. Blake, R. O. Gould, T. I. Hyde and M. Schröder, *J. Chem. Soc., Chem. Commun.*, 1987, 431; (*b*) M. Shionoya, E. Kimura and Y. Iitaka, *J. Am. Chem. Soc.*, 1990, **112**, 9237; (*c*) E. Kimura, Y. Kotake, T. Koike, M. Shionoya and M. Shiro, *Inorg. Chem.*, 1990, **29**, 4991 and references cited therein; (*d*) M. A. Hu and C. S. Chung, *J. Chin. Chem. Soc.*, 1991, **38**, 441; (*e*) K. Kobiro, A. Nakayama, T. Hiro, M. Suwa and Y. Tobe, *Inorg. Chem.*, 1992, **31**, 676; (*f*) J. R. Röper and H. Elias, *Inorg. Chem.*, 1992, **31**, 1202; (*g*) J. R. Röper and H. Elias, *Inorg. Chem.*, 1992, **31**, 1210; (*h*) M. A. Donnelly and M. Zimmer, *Inorg. Chem.*, 1999, **38**, 1650.

3 (*a*) E. Kimura,T. Koibe, H. Nada and Y. Iitaka, *Inorg. Chem.*, 1988, **27**, 1036; (*b*) E. J. Billo, P. J. Connolly, D. J. Sardella, J. P. Jasinski and R. J. Butcher, *Inorg. Chim. Acta*, 1995, **230**, 19.

4 (*a*) C. Nave and M. R. Truter, *J. Chem. Soc., Dalton Trans.*, 1974, 2351; (*b*) S. Subramanian and M. J. Zaworotko, *J. Chem. Soc., Chem. Commun.*, 1993, 952; (*c*) G. Bandoli, A. Dolmella and S. Gatto, *J. Crystallogr. Spectrosc. Res.*, 1993, **23**, 755; (*d*) S. Subramanian and M. J. Zaworotko, *Can. J. Chem.*, 1995, **73**, 414.

5 (*a*) T. W. Hambley, *J. Chem. Soc., Dalton Trans.*, 1986, 565; (*b*) R. D. Hancock, R. J. Motekaitis, J. Mashishi, I. Cukrowski, J. H. Reibenspies and A. E. Martell, *J. Chem. Soc., Perkin Trans. 2*, 1996, 1925; (*c*) K. R. Adam, I. M. Atkinson and L. F. Lindoy, *Inorg. Chem.*, 1997, **36**, 480.

6 R. Boetzel, S. Failla, P. Finocchiaro and G. Hägele, *Magn. Reson. Chem.*, 1995, **33**, 128.

7 I. Alfonso, C. Astorga, F. Rebolledo and V. Gotor, *Tetrahedron: Asymmetry*, 1999, 2515.

8 (*a*) D. F. Grant and E. J. Gabe, *J. Appl. Crystallogr.*, 1978, **11**, 114; (*b*) M. S. Lehman and F. K. Larsen, *Acta Crystallogr., Sect. A*, 1974, **30**, 580.

9 P. T. Beurskens, G. Admiraall, G. Beurskens, W. P. Bosman, S. Garcia-Granda, R. O. Gould, J. M. M. Smits and C. Smykalla, *DIRDIF user's guide. Technical report. Crystallography Laboratory*, University of Nijmegen, The Netherlands, 1992.

10 G. M. Sheldrick, *SHELXS86. In Crystallographic Computing 3*, ed. G. M. Sheldrick, C. Kruger and R. Goddard, Clarendon Press, Oxford, 1985, pp. 175–189.

11 G. M. Sheldrick, *SHELXL93. In Crystallographic Computing 6*, ed. H. D. Flack, P. Parkanyi and K. Simon, IUCr/Oxford University Press, London, 1993.

12 S. Parking, B. Moezzi and H. Hope, *J. Appl. Crystallogr.*, 1995, **28**, 53.

13 A. L. Spek, *The EUCLID package, in Computational Crystallography*, ed. D. Sayre, Clarendon Press, Oxford, 1982, p. 528.

14 International Tables for X-ray Crystallography, Vol. IV, Kynoch Press, Birmingham, 1974. (Present distributor Kluwer Academic Publishers, Dordrecht.)

15 M. Nardelli, *Comput. Chem.*, 1983, **7**, 95.

16 H. Kessler, M. Gehrke and Ch. Griesinger, *Angew. Chem., Int. Ed. Engl.*, 1988, **27**, 490.

17 MMX as implemented in PCMODEL V 5.0, Serena Software, Bloomington, IN.

18 M. Dewar, E. G. Zoebisch and E. F. Healy, *J. Am. Chem. Soc.*, 1985, **107**, 3902. Programme used: *Gaussian 94* (Revision A.1), M. J. Frisch *et al.*, Gaussian, Inc., Pittsburgh PA, 1995.

19 We have discarded the study by ^{1}H-NMR due to the complexity of the spectra. For a similar study by ^{13}C-NMR see: M. A. Bernardo, J. A. Guerrero, E. García-España, S. V. Luis, J. M. Llinares, F. Pina, J. A. Ramírez and C. Soriano, *J. Chem. Soc., Perkin Trans. 2*, 1996, 2335.

20 (*a*) P. K. Glasoe and F. A. Long, *J. Phys. Chem.*, 1960, **64**, 188; (*b*) C. Geraldes, A. D. Sherry, M. P. Marques, M. C. Alpoin and S. Cortes, *J. Chem. Soc., Perkin Trans. 2*, 1991, 137.

21 J. R. Röper and H. Elias, *Inorg. Chem.*, 1992, **31**, 1202.

22 H. Schumann, U. A. Böttger, K. Zietzke, H. Hemling, G. Kociok-Köhn, J. Pickardt, F. E. Hahn, A. Zschunke, B. Schiefner, H. Gries, B. Radüchel and J. Platzek, *Chem. Ber.*, 1997, **130**, 267.

23 (*a*) R. Taylor, O. Kennard and W. Versichel, *J. Am. Chem. Soc.*, 1984, **106**, 244; (*b*) M. C. Etter, *Acc. Chem. Res.*, 1990, **23**, 120.

24 (*a*) S. C. Wallwork, *Acta Crystallogr.*, 1962, **15**, 758; (*b*) J. L. Sessler, E. A. Brucker, V. Lynch, M. Choe, S. Sorey and E. Vogel, *Chem. Eur. J.*, 1996, **2**, 1527.

25 (*a*) H. Günther, *NMR Spectroscopy: Basic Principles Concepts and Applications in Chemistry*; John Wiley and Sons, Chichester, 2nd edn., 1995, pp. 80–81; (*b*) F.-A. Kang and Ch.-L. Yin, *J. Am. Chem. Soc.*, 1997, **119**, 8562.

26 Stabilization of protonated species by interactions with halide anions in polar solvents have been observed in macrocyclic and macrobicyclic polyamines: (*a*) M. W. Hosseini and J.-M. Lehn, *Helv. Chim. Acta*, 1988, **71**, 749; (*b*) B. Dietrich, B. Dilworth, J.-M. Lehn, J.-P. Souchez, M. Cesario, J. Guilhem and C. Pascard, *Helv. Chim. Acta*, 1996, **79**, 569; (*c*) F. P. Schmidtchen and M. Berger, *Chem. Rev.*, 1997, **97**, 1609.

27 For FABMS based studies of some ionic complexes see: (*a*) M. Sawada, Y. Okumura, M. Shizuma, Y. Takai, Y. Hidaka, H. Yamada, T. Tanaka, T. Kaneda, K. Hirose, S. Misumi and S. Takahashi, *J. Am. Chem. Soc.*, 1993, **115**, 7381.

28 I. Alfonso, F. Rebolledo and V. Gotor, *Tetrahedron: Asymmetry*, 1999, 367.

Paper a904998c